Supporting Information

Solvent- and concentration-induced self-assembly of an amphiphilic perylene dye

Antonella Caterina Boccia,[a] Vladimir Lukes [b] Anita Eckstein-Andicsovà, [c] and Erika Kozma [a]

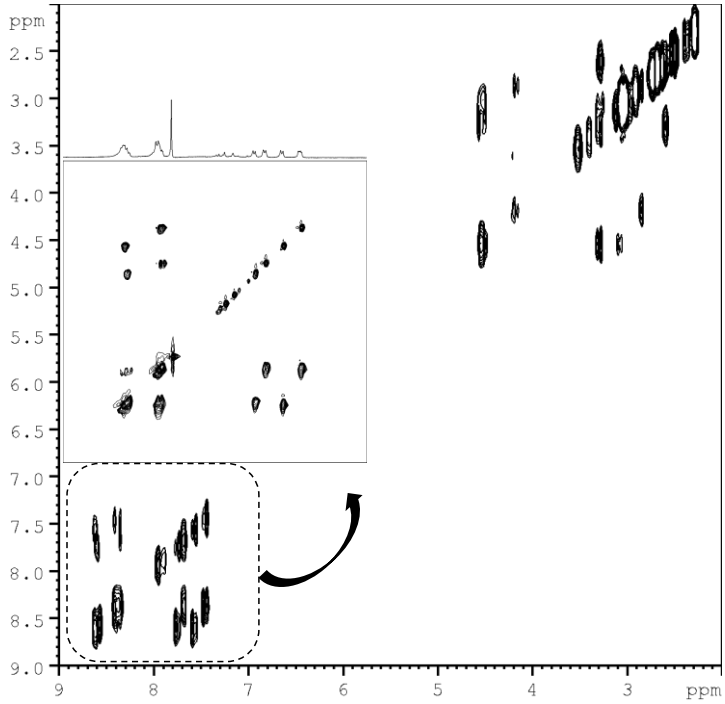

Fig. S1 ESI. 2D COSY spectrum of **PDA-CA** in DMSO, $2.1 \cdot 10^{-2}$ M, 298 K

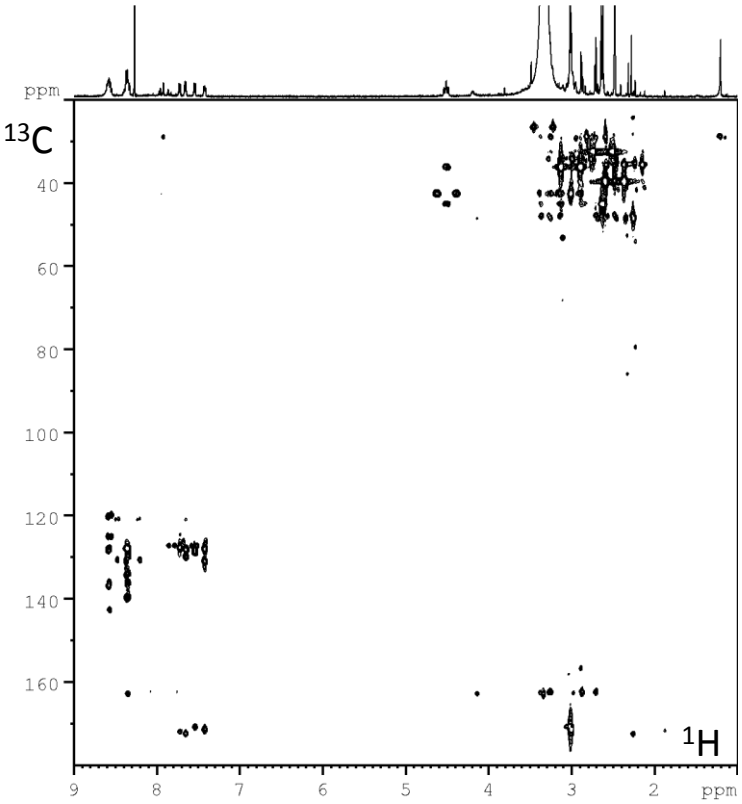

Fig. S2 ESI. HMBC spectrum of **PDA-CA** in DMSO, $2.1 \cdot 10^{-2}$ M, 298 K

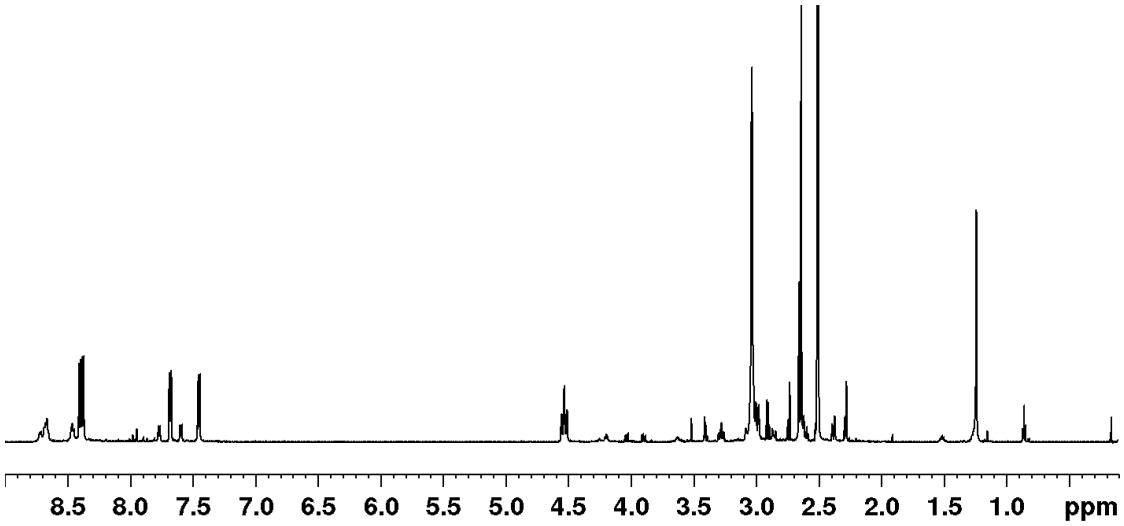

Fig. S3 ESI. ^{1}H NMR spectrum of **PDA-CA** in DMSO, $2.1 \cdot 10^{-2}$ M, (full spectrum).

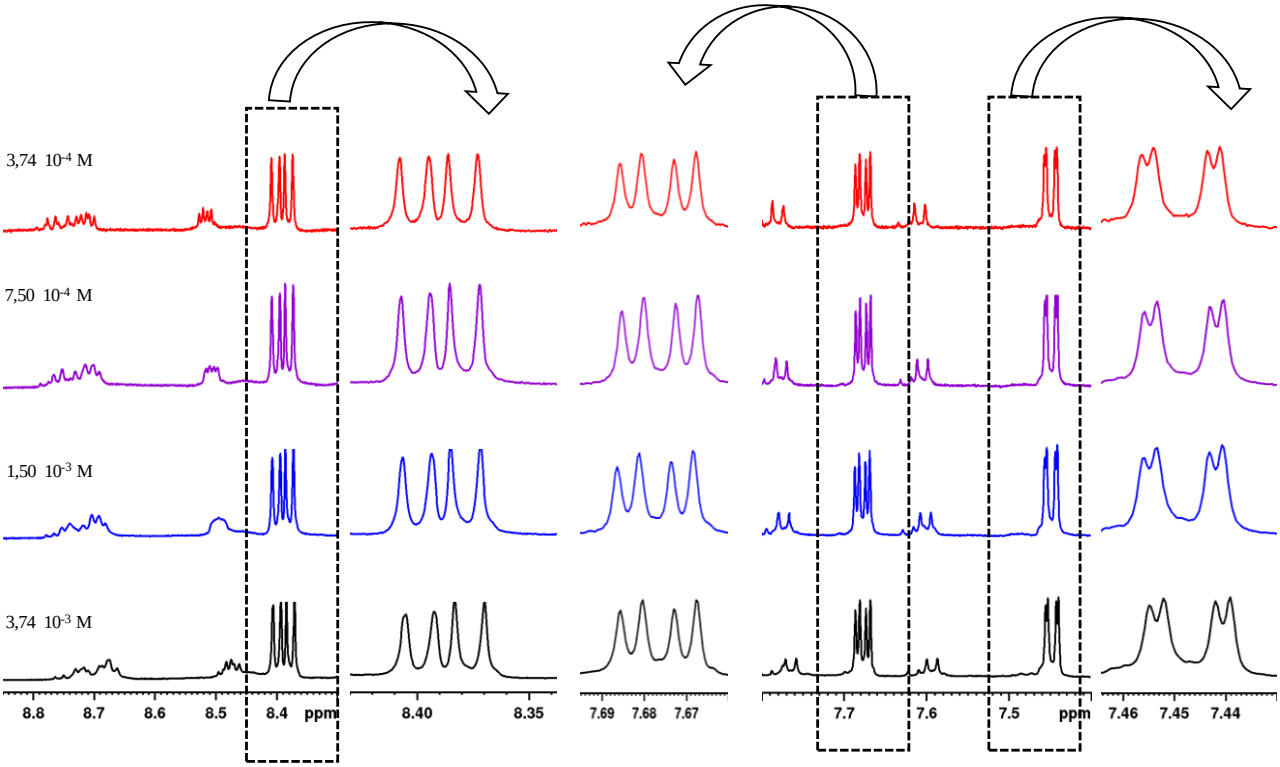

Fig. S4 ESI. Variable-concentration ^{1}H NMR measurement of PDA-CA at 298 K, in DMSO.

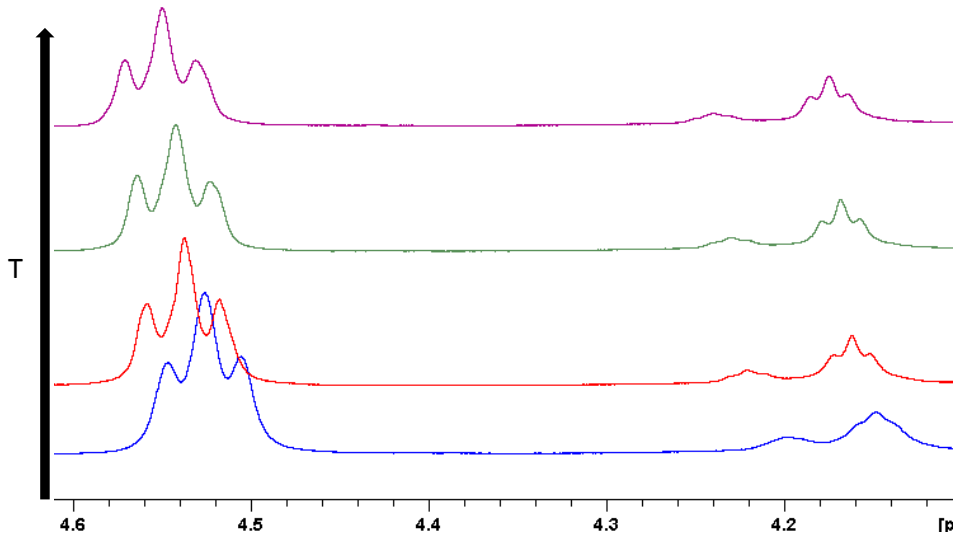

Fig. S5 ESI. ^{1}H NMR spectra of **PDA-CA** methylene signal bonded to N ($2.1 \cdot 10^{-2}$ M), at variable temperature, in DMSO.

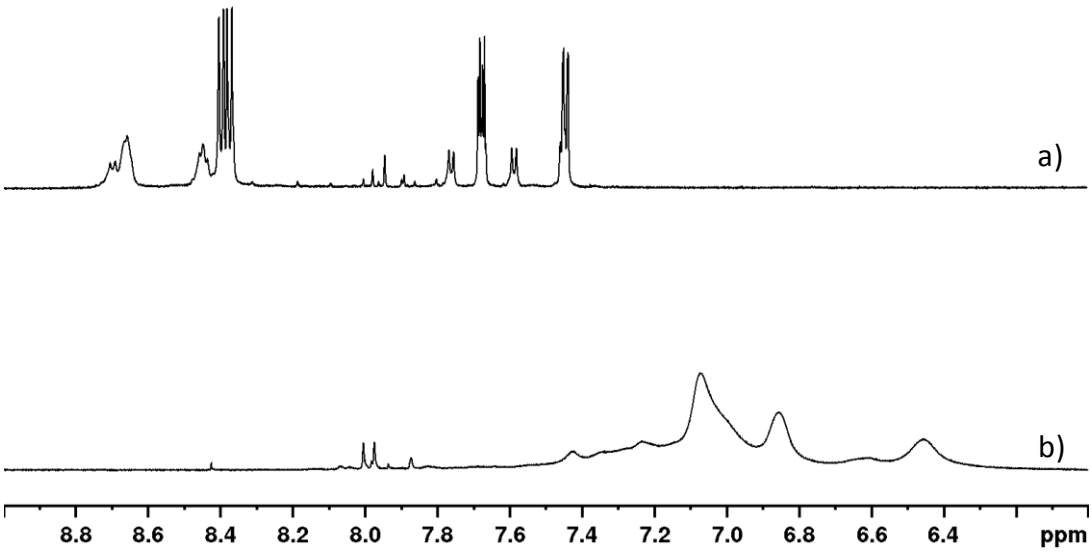

Fig. S6 ESI. ^{1}H NMR spectra of expanded aromatic region of **PDA-CA** ($7.0 \cdot 10^{-3}$ M), in: a) DMSO; b) D_2O.

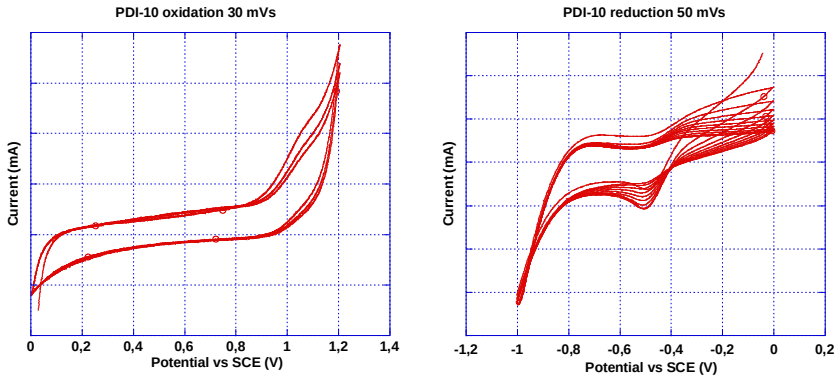

Fig. S7 ESI. Cyclic voltammetry of **PDA-CA** in sodium sulfate 0.1M solution

Cyclic voltammetry measurements were performed in solution, under nitrogen atmosphere with a computer controlled Amel 2053 (with Amel 7800 interface) electrochemical workstation in a three electrode single-compartment cell using platinum electrodes and SCE as standard electrode, with Fc/Fc+ redox couple as internal standard, with a sodium sulfate solution (0.1M) in water at a scan rate of 50 $mV \cdot s^{-1}$.

Conformation	Gas	DMSO	Water
syn-a			
E_{ele} / hartree H / hartree	–1909.339663 –1908.738219	–1909.380618 –1908.779984	–1909.386761 –1908.787275
syn-b			
E_{ele} / hartree H / hartree	–1909.326605 –1908.726871	–1909.371838 –1908.772009	–1909.380860 –1908.779766
ΔE_{ele} / kJ·mol^{-1}	34.2	23.0	15.5
ΔH / kJ·mol^{-1}	29.8	20.9	19.7

Conformation	Gas	DMSO	Water
anti-a			
E_{ele} / hartree H / hartree	–1909.333988 –1908.733064	–1909.380685 –1908.779359	–1909.387066 –1908.784021
anti-b			
E_{ele} / hartree H / hartree	–1909.324151 –1908.724257	–1909.368613 –1908.769820	–1909.374316 –1908.772826
ΔE_{ele} / kJ·mol^{-1}	25.8	31.7	33.4
ΔH / kJ·mol^{-1}	23.1	25.0	29.4

Fig. S8 ESI. The B3LYP/6-31G(d,p) electronic energies (E_{ele}), enthalpies (H) and Gibb´s free energies (G) calculated for the gas-phase, DMSO and water environment. The energy differences are calculated with respect to the closed conformation.

	Gas	DMSO	Water
syn-a			
$S_0 \rightarrow S_1$	481 nm (0.505)	492 nm (0.730)	488 nm (0.743)
$S_0 \rightarrow S_2$	474 nm (0.000)	436 nm (0.007)	418 nm (0.003)
$S_0 \rightarrow S_3$	474 nm (0.084)	436 nm (0.000)	417 nm (0.000)
$S_0 \rightarrow S_4$	376 nm (0.001)	366 nm (0.005)	351 nm (0.011)
$S_0 \rightarrow S_5$	376 nm (0.014)	363 nm (0.000)	346 nm (0.004)
syn-b			
$S_0 \rightarrow S_1$	477 nm (0.579)	489 nm (0.722)	487 nm (0.735)
$S_0 \rightarrow S_2$	427 nm (0.002)	401 nm (0.001)	395 nm (0.001)
$S_0 \rightarrow S_3$	426 nm (0.000)	401 nm (0.000)	395 nm (0.000)
$S_0 \rightarrow S_4$	392 nm (0.001)	379 nm (0.000)	356 nm (0.000)
$S_0 \rightarrow S_5$	389 nm (0.017)	377 nm (0.008)	356 nm (0.004)

Conformation	Gas	DMSO	Water
anti-a			
$S_0 \rightarrow S_1$	473 nm (0.164)	487 nm (0.780)	487 nm (0.766)
$S_0 \rightarrow S_2$	473 nm (0.000)	436 nm (0.001)	420 nm (0.001)
$S_0 \rightarrow S_3$	472 nm (0.477)	435 nm (0.002)	420 nm (0.000)
$S_0 \rightarrow S_4$	378 nm (0.001)	366 nm (0.000)	355 nm (0.001)
$S_0 \rightarrow S_5$	374 nm (0.000)	362 nm (0.001)	349 nm (0.000)
anti-b			
$S_0 \rightarrow S_1$	469 nm (0.615)	485 nm (0.735)	481 nm (0.748)
$S_0 \rightarrow S_2$	422 nm (0.000)	393 nm (0.000)	393 nm (0.000)
$S_0 \rightarrow S_3$	422 nm (0.000)	393 nm (0.000)	392 nm (0.000)
$S_0 \rightarrow S_4$	378 nm (0.001)	375 nm (0.000)	350 nm (0.000)
$S_0 \rightarrow S_5$	377 nm (0.003)	373 nm (0.002)	347 nm (0.000)

Fig. S9 ESI. The TD-B3LYP/6-31G(d,p) optical transitions of *syn*- and *anti*-isomers calculated for gas-phase and solvent environments. The values in parentheses stand for the oscillator strengths.

	D(syn-a)		D(anti-a)		D(syn/anti-a)
$S_0 \rightarrow S_1$	559 nm (0.018)		564 nm (0.027)		573 nm (0.016)
$S_0 \rightarrow S_2$	558 nm (0.018)		553 nm (0.006)		549 nm (0.022)
$S_0 \rightarrow S_3$	482 nm (0.349)		480 nm (0.434)		480 nm (0.371)
$S_0 \rightarrow S_4$	482 nm (0.390)		474 nm (0.323)		482 nm (0.351)
$S_0 \rightarrow S_5$	447 nm (0.001)		427 nm (0.001)		433 nm (0.001)
$S_0 \rightarrow S_6$	447 nm (0.002)		427 nm (0.005)		428 nm (0.003)
$S_0 \rightarrow S_7$	438 nm (0.002)		426 nm (0.001)		425 nm (0.001)
$S_0 \rightarrow S_8$	436 nm (0.002)		426 nm (0.000)		418 nm (0.000)
$S_0 \rightarrow S_9$	434 nm (0.000)		409 nm (0.000)		416 nm (0.000)
$S_0 \rightarrow S_{10}$	434 nm (0.000)		408 nm (0.000)		413 nm (0.001)

Fig. S10 ESI. The gas-phase TD-B3LYP/6-31G(d,p) optical transitions of model π-dimers. The values in parentheses stand for the oscillator strengths.

$S_0 \rightarrow S_1$: **2.20 eV / 564 nm, *f* = *0.027***

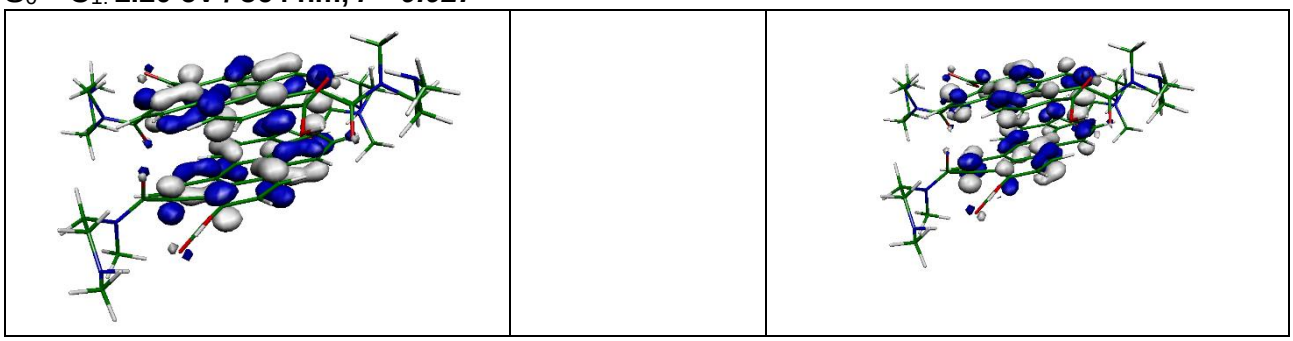

HOMO → LUMO (83%)

$S_0 \rightarrow S_2$: **2.24 eV / 553 nm, *f* = *0.006***

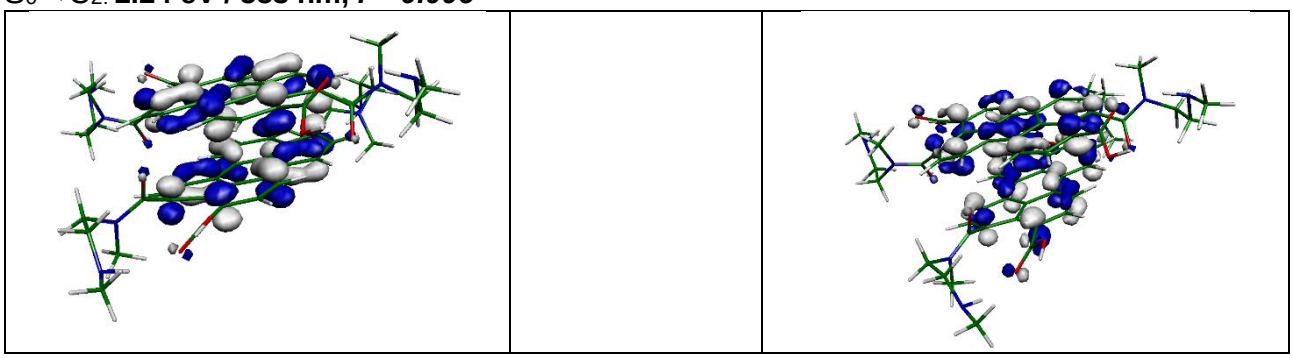

HOMO → LUMO+1 (63%)

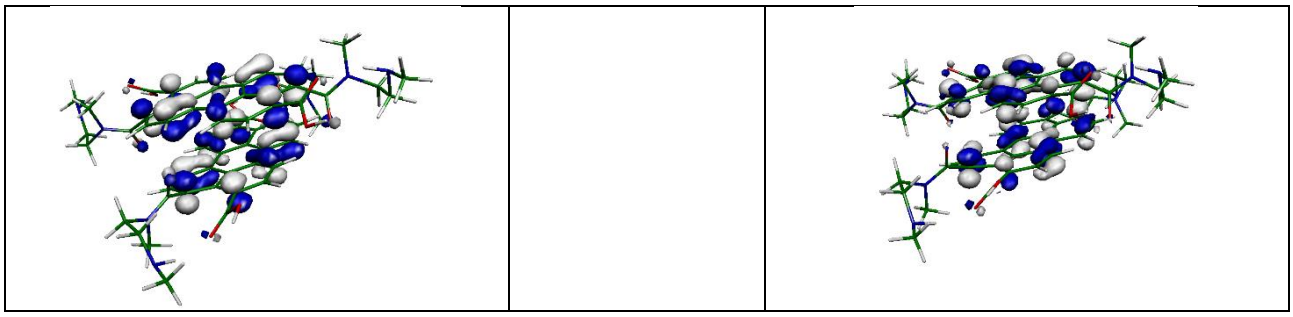

HOMO–1 → LUMO (37%)

$S_0 \rightarrow S_3$: **2.59 eV / 480 nm, *f* = *0.443***

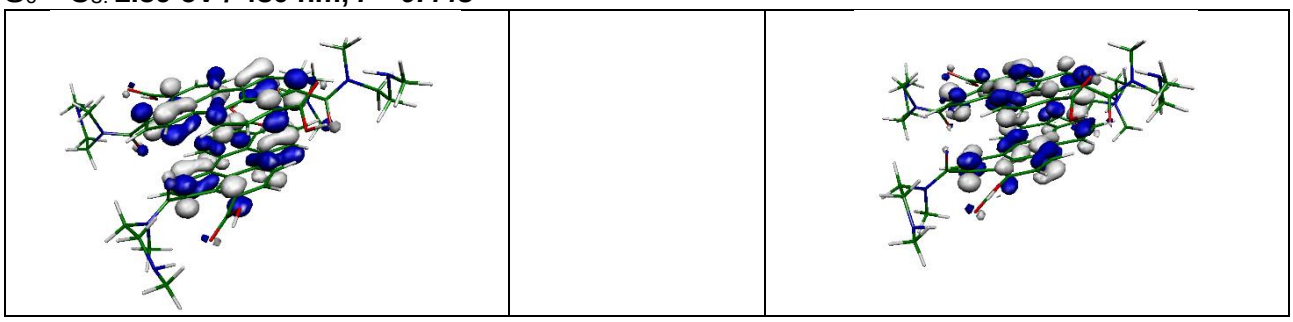

HOMO–1 → LUMO (63%)

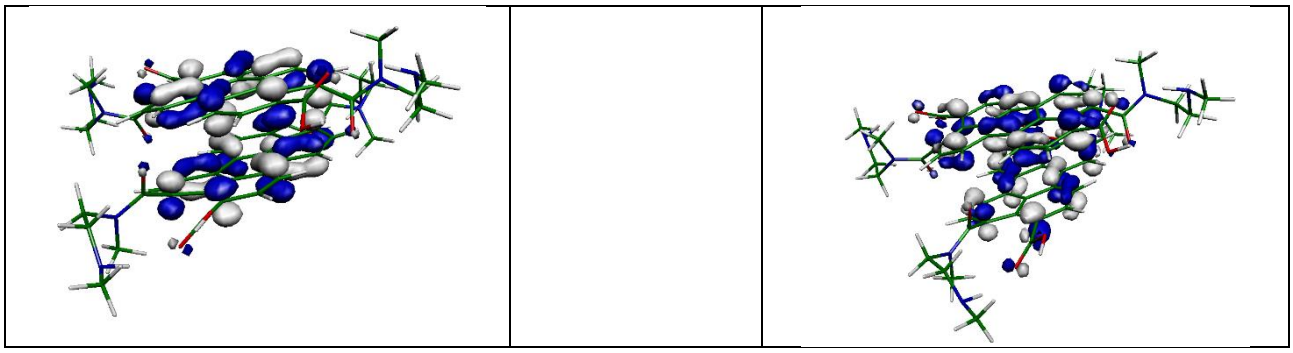

HOMO → LUMO+1 (37%)

$S_0 \rightarrow S_4$: **2.60 eV / 478 nm, *f* = *0.339***

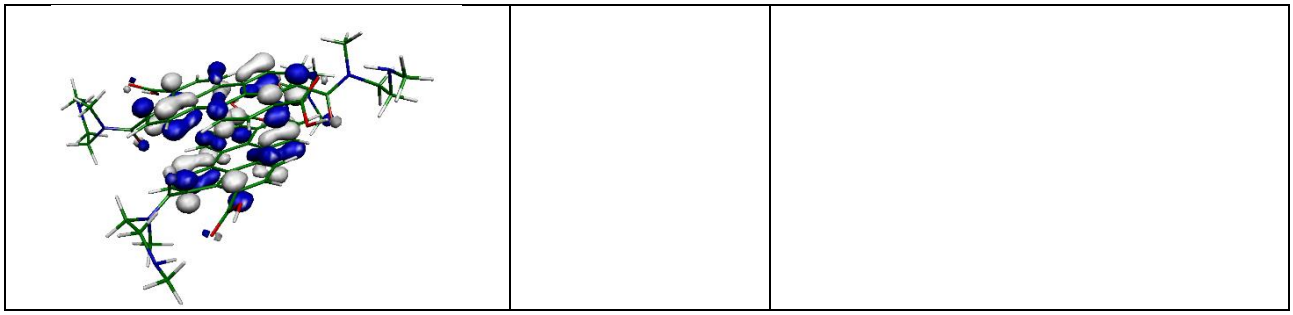

HOMO–1 → LUMO+1 (82%)

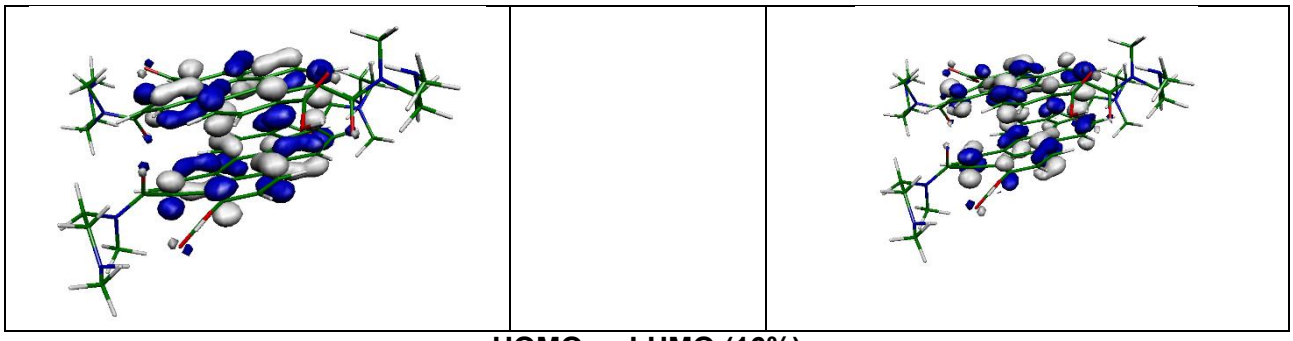

HOMO → LUMO (16%)

Fig. S11 ESI. Plots of the B3LYP/6-31G(d,p) molecular orbitals significantly contributing to the first four gas-phase lowest energy TD-B3LYP optical transitions for symmetric **D(anti-a)** π-dimer. The values in parentheses stand for percentages of excitation contributions in individual transitions. The value of the depicted isosurface is 0.035 bohr$^{-3/2}$. The symbol *f* denotes oscillator strength.

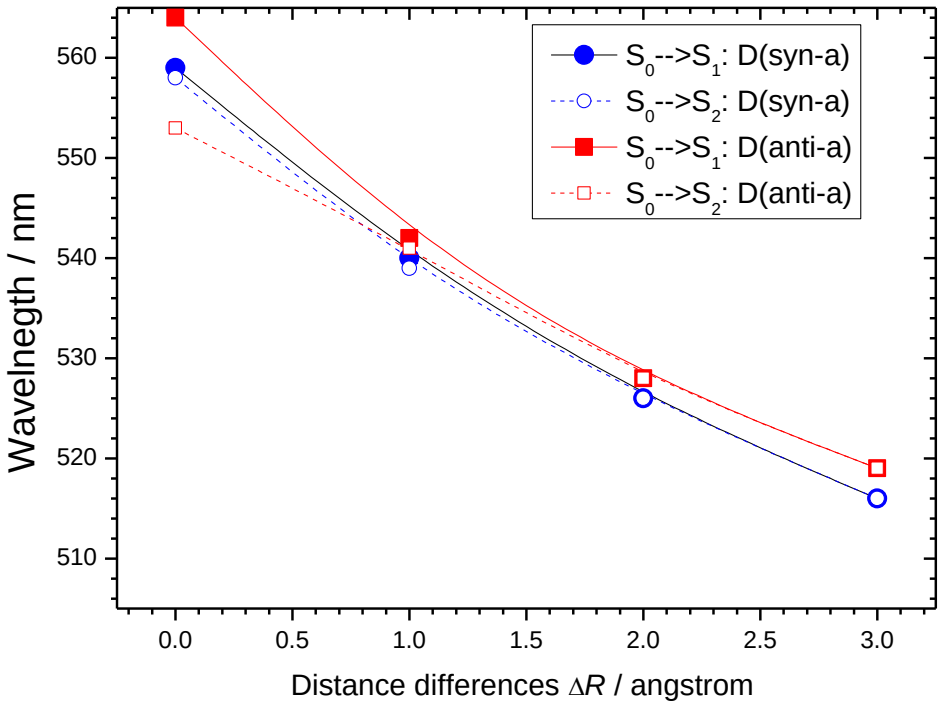

Fig. S12 ESI. The dependence of the two lowest gas-phase TD-B3LYP//B3LYP-D/6-31G(d,p) energy optical transitions on the interplane distances displacement of rigid monomers for model **D(syn-a)** (a) and **D(anti-a)** (b) π-dimers. The distance difference Δ*R* is defined with respect to the gas-phase equilibrium interplane distances 3.38 Å for **D(syn-a)** dimer and 3.39 Å for **D(anti-a)** dimer.

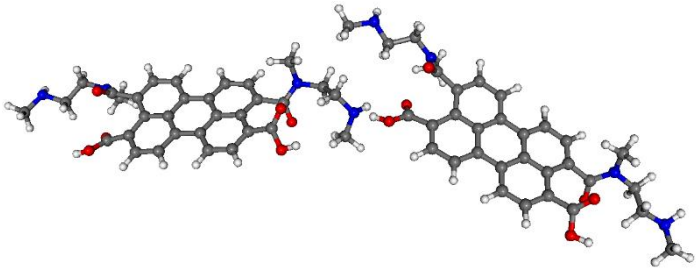

Fig. S13 ESI. The B3LYP-D optimal gas-phase geometry of model hydrogen-bonded H-dimer consisting of two **syn-b** molecules.